Analyst

Accepted Manuscript

ROYAL SOCIETY OF CHEMISTRY

www.rsc.org/analyst

FTIR Imaging of Structural Changes in Visceral and Subcutaneous Adiposity and Brown to White Adipocyte Transdifferantiation

Fatma KUCUK BALOGLU[1],Sebnem GARIP[2],Sebastian HEISE[3], Gudrun BROCKMANN[3], Feride SEVERCAN[1*]

[1]Department of Biological Sciences, Middle East Technical University, Ankara, Turkey

[2]Department of Medical Biochemistry, Faculty of Medicine, Istanbul Kemerburgaz University, Istanbul, Turkey

[3]Department of Breeding Biology and Molecular Genetics, Humboldt Universitatzu Berlin, Berlin, Germany

*Corresponding Author: Feride Severcan

Department of Biological Sciences

Middle East Technical University

06531, Ankara, TURKEY

Tel: +90-312-210 51 66

Fax: +90-312-210 79 76

E-mail: feride@metu.edu.tr

Abstract

Obesity is a heterogeneous disorder which increases risks for multiple metabolic diseases, such as type 2 diabetes. The current study aims to characterize and compare visceral and subcutaneous adipose tissues in terms of macromolecular content and investigate transdifferentiation between white and brown adipocytes. Regarding this aim, Fourier transform infrared (FTIR) microspectroscopy and uncoupling protein 1 (UCP1) immunohistological staining was used to investigate gonadal (visceral) and inguinal (subcutaneous) adipose tissues of male Berlin fat mice inbred (BFMI) lines, which are spontaneously obese. The results indicated a remarkable increase in the lipid/ protein ratio, accompanied with a decrease of UCP1 protein content which might be due to the transdifferentiation of brown adipocytes to white adipocytes in obese groups. It has been widely reported that brown adipose tissue has a strong effect on fatty acid and glucose homeostasis and it could provide opportunity for therapy of obesity. When the amount of brown adipose tissue was decreased, lower unsaturation/saturation ratio, qualitatively longer hydrocarbon acyl chain length of lipids and higher amount of triglycerides were obtained in both adipose tissues of mice lines. The results also revealed that subcutaneous adipose tissue was more prone to obesity-induced structural changes, than visceral adipose tissue, which could be originated from possessing a lower amount of brown adipose tissue. The current study clearly revealed the power of FTIR microspectroscopy in the precise determination of obesity-induced structural and functional changes in inguinal and gonadal adipose tissue of mice lines.

Keywords: Obesity, visceral adipose tissue, subcutaneous adipose tissue, white adipose tissue, brown adipose tissue, UCP1 protein, FTIR imaging, transdifferentiation.

1. Introduction

Obesity results from a prolonged imbalance between the level of energy intake and expenditure leading to excessive weight gain. It is also referred to as an epidemic disease caused by the modern life style which affects increasing number of people of all social conditions throughout the world.[1] Obesity is becoming one of the major public health problems. The World Health Organization reported that more than 1.4 billion adults were overweight and over 200 million men and nearly 300 million women of them were obese. [2] Epidemiologic studies estimate that by the year 2030, 2.16 billion people worldwide will be overweight and 1.12 billion will be obese.[3] Obesity results in accumulation of triglycerides in adipose tissues and the enlargement of adipocytes.[4] An excessive accumulation of lipid droplets in cytoplasm may lead to cellular dysfunction or cell death, a phenomenon known as lipotoxicity. [5,6]

Adipose tissue is an essential, complex and metabolically active endocrine organ which is distributed in a variety of locations in the body different than the other organs. [7,8] Adipose tissue depots are composed of two cytotypes. These cytotypes are white adipose tissue and brown adipose tissue. White adipocytes are spherical cells whose variable size mainly depends on the size of the single lipid droplet stored in them. This lipid droplet consists of triglycerides and accounts for more than 90% of the cell volume. Brown adipocytes also contain triglycerides as multiple small vacuoles; they are typically polygonal with a variable diameter. The most characteristic organelles of brown adipocytes are the mitochondria. Because of its greater oxygen demand, brown fat also contains more capillaries than white fat. Nerve supply is also denser in brown adipose tissue than in white adipose tissue. The brown color of brown adipocytes is attributable to its high mitochondrial density and high vascularization. [9,10] The amount of these two types of adipose tissues in the body shows variety according to strain, gender, age, nutritional environmental factors. Brown adipocytes

have a completely different role than white adipocytes since they are responsible for thermogenesis. They transfer the energy achieved from nutrition to thermal energy. [11,12]

Uncoupling protein 1 (UCP1), which is mostly expressed in brown adipose tissue, is responsible for the transformation of the energy that is not used in oxidative metabolism into heat.[13] Noradrenaline is responsible for the activation of beta-3-adrenoceptors which induces brown adipocytes to produce heat. When brown adipocytes are not stimulated adrenergically, they lose most of their brown characteristics and transdifferentiate into white adipocytes.[14,15] This reversible morphological transformation occurs with leptin gene activation and UCP-1 gene inhibition.[16] In rodents, brown adipose tissue phenotype in adipose tissues is very important for the prevention of many metabolic diseases such as obesity and diabetes. [14]

FTIR spectroscopy was previously applied to obesity research for determination of fatty acid content in human abdominal fat,[17] and recently to high fat diet induced obesity in BXD recombinant inbred mice lines to identify specific gene loci responsible for the variations in the molecular tissue compositions.[18] In the current study, FTIR microspectroscopy was applied to identify spontaneous obesity-induced molecular changes in adipose tissues of inbred obese mice lines. Fourier transform infrared (FTIR) microspectroscopy enables the visualization of the distribution of molecules in a tissue.[19-22] Due to the sensitivity of FTIR microspectroscopy and the information on spatial heterogeneity possessed in the images, IR spectral images give information on the histological structure of the tissue without the application of staining procedures.[23] In this technique, every pixel includes a spectrum which is recorded sequentially, and the pixels are collected together to form a larger image. The recorded information by IR microscopy is represented by false-color images that simulates the images as histological-stained samples.[24]

In this study, FTIR microspectroscopic imaging was performed to determine the distribution of molecules, especially lipids, in two different adipose tissues; inguinal adipose tissue as a

subcutaneous adipose tissue, gonadal adipose tissue as a visceral adipose tissue, and also to figure out the obesity-induced structural variations in the lipids. For this purpose, inguinal and gonadal adipose tissues of control (DBA/J2) and spontaneous obese (BFMI) lines were used. In addition, UCP1 immunohistological staining was performed to differentiate brown adipose tissue and white adipose tissue; so transdifferentiation between brown and white adipocytes of these tissues were investigated.

2. Experimental

2.1 *Animals*

All experimental protocols regarding treatment of animals were approved by the German Animal Welfare Authorities (approval no. G0171/10). Founder animals of the Berlin Fat Mice lines were originally purchased from several pet shops in Berlin, Germany. These mice were selected during 58 generations, according to low protein content and then to low body weight and high fat content. Then, BFMI line's inbred derivates were generated and these lines were created by brother and sister mated randomly chosen sib-pairs of the selected lines.[25]

In this study, 10 weeks old males of BFMI852, BFMI856, BFMI860 and BFMI861 inbred lines which were separated in terms of phenotypic characteristics after six generations of inbreeding, were used. Due to the selection history of the lines, different genetic constellations have been fixed in the process of inbreeding leading to major differences in the phenotype. There are significant differences between BFMI lines in terms of body fat mass, body fat percentage, weights of dissected fat pads, inner organs and glucose concentrations.[25] BFMI lines 856, 861 and 860 are the most obese lines, whereas only 860 and 861 show features of the metabolic syndrome and reduced insulin sensitivity. It has been reported that BFMI860 line has higher serum triglyceride levels in both standard breeding diet and high fat diet.[26] As controls male DBA/J2 mice line was used, which is a commercially available inbred

line that is often used as a standard mice showing a wildtype-like phenotype.[27,28] In the study, each group contained 6 mice.

The mice were maintained under conventional conditions and controlled lighting with a 12:12h light/dark cycle at a temperature of 22±2°C and a relative humidity of 65%. They were reared in groups of two to three mice in macrolon cages with a 350 cm^2 floor space (E. Becker & Co (Ebeco) GmbH, Castrop-Rauxel, Germany) and with dust-free bedding type S80/150 (Rettenmeier Holding AG, Wilburgstetten, Germany). All mice had *ad libitum* access to food and water. After weaning at the age of 3 weeks, animals were fed with a rodent standard breeding diet (SBD). The SBD (V1534-000, ssniff R/M-H, Ssniff Spezialdiäten GmbH, Soest/Germany) contains 12.8 MJ/kg of metabolisable energy the biggest amount of which originates from carbohydrates with 58% (33% from proteins and 9% from fat). The fat content of SBD was derived from soy oil.[26]

2.2 *Sample preparation*

After 10 weeks, mice were killed by decapitation, inguinal and gonadal adipose tissues of the mice were dissected and washed with PBS buffer to get rid of the excess blood surrounding the tissue. They were snap-frozen in liquid nitrogen and stored at -80ºC until sectioning. Three sections were prepared for each sample. For sectioning, the adipose tissue samples were embedded in Cryomatrix Frozen Embedding Medium (Thermo Scientific, USA). 7 µm thick adjacent tissue sections were obtained using a cryotome (Shandon, USA) at -25°C both for FTIR microspectroscopy and immunohistological studies. The tissue sections for FTIR study were directly transferred onto IR transparent barium fluoride windows (Spectral Systems, NY, USA). These IR sections were kept in a desiccator with a vacuum pump at cold room for overnight to remove the moisture from the sections.

2.3 *Immunohistological staining*

The Inguinal and gonadal adipose tissues of BFMI lines and control DBA/J2 line have been used for UCP1 immunohistological staining in order to differentiate brown and white adipose tissues for the monitoring of transdifferentiation. For staining "EXPOSE rabbit specific AP (red) detection IHC Kit" (Abcam, USA) and Biotin goat anti rabbit antibody (Vector Lab. Inc., USA) were used. Immunohistological staining was applied as described in the kit procedure. After drying for overnight in desiccator, slides were treated with acetone at -20°C and waited for 10 minutes at -20°C and then washed 3 times in buffer (PBS). Then, we applied Protein Block and incubated the slides for 10 minutes at room temperature to block nonspecific background staining and wash 3 times in buffer again. In next step, we applied primary antibody (Biotin goat anti rabbit antibody (Vector Lab. Inc., USA)) and incubated the slides according to manufacturer's protocol and washed 3 times in buffer. After that, AP conjugate was applied and the slides were incubated for 30 minutes at room temperature and rinsed 4 times in buffer. The 200 µl of enhancer was applied to the slides and the slides were incubated for 4 minutes at room temperature. We mixed equal volume of Naphthol Phosphate and Fast Red just before using, and then applied 200 µl of this mixture onto the slides with Enhancer. The recommended incubation time was 8 minutes at room temperature. Then, the slides were rinced 4 times in buffer followed by Hematoxylin staining as a counter-staining. For counter-staining, Hematoxylin was added to cover the slides which were then incubated for 1 minute and they were 7-8 times in tap water. Stained slides were made permanent by Eukitt® quick-hardening mounting medium (Sigma-Aldrich, USA) and they were quantified by observing with a light microscope under 40X magnification.

2.4 FTIR Microspectroscopic Data Collection and Analysis

FTIR images were acquired using a Perkin Elmer Spectrum Spotlight 400 Imaging System (Perkin Elmer Instruments, Boston, MA, USA), including an IR microscope. Images were collected in the transmission mode at a spectral resolution of 8 cm^{-1} in the wavenumber region between 4000 and 750 cm^{-1} with a 6.25× 6.25 μm IR detector pixel size and four scan number per pixel. Although, adipose tissue is a highly homogenious tissue, we randomly chose three different areas in each tissue section to collect IR maps. FTIR microscope collects these IR images by scanning the chosen areas pixel by pixel (pixel size: 6.25 x 6.25μm) and getting an IR spectrum from each pixel. The size of the spot or pixel was determined by the size of the microscope aperture which might be defined as micrometers. Since the size of the collected IR maps is 700x700μm, totally 12544 spectra were recorded from each chosen area of each section. Before calculating the spectral parameters, first the average of 12544 spectra was taken from each area. The average spectra of each area were found to be almost identical. Then the average spectrum of these three average spectra belong to the chosen areas was used for each section for further analysis. Thus, the spectral alterations between animal groups reflect cellular alterations rather than experimental uncertainties. The spectra of empty IR window were collected as background and subtracted automatically from tissue spectra by the use of Spotlight Autoimage software (Perkin Elmer Instruments, Boston, MA, USA).

In FTIR microspectroscopic studies of tissues, the main parameter which can affect the results of cellular alterations is sample thickness. In the analysis of FTIR images, band area ratios were used in order to avoid the errors that might occur due to possible differences in section thickness which may **cause** concentration-dependent alterations in the spectral absorbance values.[29-31] Spectral images were analyzed using ISYS software (Spectral Dimensions, Olney, MD, USA).

2.5 *Statistics*

The results were calculated as 'mean ± standard error of mean (SE)'. The differences in variance were analyzed statistically using one-way ANOVA test. Tukey's test was used as a post-hoc test. p values less than or equal to 0.05 were considered as statistically significant (such as $*p \leq 0.05$; $**p \leq 0.01$; $***p \leq 0.001$).

3. Results

Biological samples contain different molecules such as proteins, lipids, nucleic acids and carbohydrates. Hence, all these individual biochemical components have their specific vibrational fingerprints.[32-34] By using this property, FTIR microspectroscopic imaging enables to obtain visible images of the investigated tissue, where each pixel is composed of a spectrum originating from vibrational fingerprints. The representative FTIR spectra acquired from control (DBA/J2) and obese (BFMI861) groups of inguinal adipose tissue in the 4000–750 cm^{-1} region are shown in Figure 1. The detailed spectral band assignments of mouse adipose tissue are shown in Table 1.[18,35,36]

In order to determine obesity-induced alterations in the concentration and composition of biomolecules, the area ratios of several functional groups that belong to lipids and proteins were calculated. The wavenumber limits with baseline points used for the band area ratio calculations for each vibrational region, were given in Table 1S as a supporting material. The lipid to protein ratio is an important parameter in molecular asymmetry.[37] This ratio was obtained by taking the ratio of the integrated areas of C-H stretching region to the area of the amide I band. The C-H stretching region which contains significant vibrations of the fatty acyl chains of membrane lipids is a sensitive marker for the lipid content.[38-40] Amide I band gives information about total protein concentration and conformation.[21,41]

In order to obtain qualitative information on lipid structure of adipose tissues, carbonyl/lipid and unsaturated/saturated lipid ratio were calculated. Carbonyl/lipid ratio was calculated by taking the ratio of the area of carbonyl band to that of C-H stretching region. Unsaturated/saturated ratio was calculated by taking the ratio of the area of the olefinic band (unsaturated lipid) to that of CH_2 antisymmetric band (saturated lipid). Qualitative lipid acyl chain length changes were monitored by calculating the ratio of areas of the CH_2 antisymmetric band to that of the CH_3 antisymmetric band. Furthermore, lipid and protein amounts were obtained from CH_2 symmetric/CH_2 antisymmetric and the amide I/ amide I + amide II ratios, respectively. The comparison of these ratios in terms of bar graphs for the control (DBA/J2) and 4 different obese (BFMI) male mice lines are shown in figure 2. As seen from these graphs, the lipid/protein ratio, carbonyl/lipid ratio, lipid amount (CH_2 symmetric/CH_2 antisymmetric) and qualitative lipid acyl chain length changes (CH_2/CH_3 antisymmetric) increased; whereas unsaturated/saturated lipid ratio (olefinic/lipid) and protein amount (amide I/ amide I + amide II) decreased for obese male mice lines when they were compared with the control (DBA/J2) line.

The significant increase in the lipid/protein ratio in the obese groups compared to the control, might be due to the dramatic increase in the lipid content as seen from CH_2 symmetric/CH_2 antisymmetric ratio and/or from the significant decrease in protein content that we observed in obese lines.[40] The increase in the lipid/protein ratio was more remarkable in inguinal adipose tissue rather than gonadal adipose tissue. This might be due to that inguinal adipose tissue is prone to deposite lipids rather than gonadal tissue because inguinal tissue is a subcutenous adipose tissue, whereas gonadal tissue is a visceral adipose tissue.[42] The increase of lipid/protein ratio in obese groups may also be arised from a lower protein content. The changes in amide I area/intensity values give information about total protein amount.[34] We obtained a significant decrease in the band area value of the amide I of adipose tissues of

obese groups implying a decrease of protein content in harmony with literature values (Table 2). Decrease in protein content was also supported by the significant decrease of amide I/ amide I + amide II ratio (Figure 2). To obtain more information about changes in protein composition and structure, we calculated the band area ratio of amide I/ amide II (Figure 2). This ratio decreased in obese lines compared to the control group. Since amide I and amide II profiles depend on the protein structural composition, this decrease suggests that there are some alterations in the structures of proteins.[43-45] In addition' slight but significant shifting in the wavenumber of amide I band to higher values wasobserved in the all obese groups in comparison to the control group (Table 2) which indicates alterations in protein conformation.[46-48] The changes in the spectral parameters related to protein such as; the decrease in the area of amide I band and amide I/amide II band area ratio, and the shifting of the amide I band to higher wavenumber values, could be interpreted as a result of the alteration of protein expression which may cause obesity-induced changes in protein structure and conformation in adipose tissues.

The olefinic/lipid ratio can be used as an index of double bonds in the lipid structure indicating the relative amount of unsaturated lipids.[21,38] The significant decrease in olefinic/lipid ratio was observed in all obese mice lines compared to the control group, indicating that unsaturated lipid content decreased in obese mice lines. This ratio was also lower in inguinal adipose tissue rather than in gonadal adipose tissue of all groups.

The carbonyl/lipid ratio gives information about carbonyl ester concentration in lipids of the system.[21,49,50] This ratio was slightly higher in BFMI852 and BFMI856 lines but significantly higher in BFMI 860 and BFMI861 lines.

The CH_2 antisymmetric stretching/CH_3 antisymmetric stretching ratio was used to determine the qualitative changes in hydrocarbon acyl chain length of lipids, where higher ratios indicate the presence of longer chained lipids.[34,39,51-53] We obtained an increase in this ratio in all obese

BFMI lines but they were only significant for BFMI860 and BFMI861 lines. The ratio was also more significant in inguinal adipose tissue than gonadal adipose tissue in numerous of lines as seen from figure 2. In order to get information about qualitative lipid acyl chain lengths changes, the ratio of the area of CH_2 antisymmetric stretching band to lipid (C-H region) was also calculated. The increased ratio values obtained from this ratio also supported relative variations towards to longer acyl chain lengths of lipids in obese mice groups compared to the control.[21,54]

The representative spectral maps of lipid/protein, olefinic/protein and CH_2/CH_3 antisymmetric ratios of inguinal adipose tissue of control (DBA/J2) and obese (BFMI861) male mice line were shown in Figure 3 for both tissue types. Since the obesity-induced changes were seen more dramatically for inguinal adipose tissue of BFMI861 line as seen from Figure 2, the comparison of FTIR images of this line with the control was presented in Figure 3. The spectral maps are represented as color-coded images which are composed of a spectrum in each pixel and they were colored according to the calculated ratio values, where red color corresponds to the highest ratio and blue color corresponds to the lowest ratio as shown on the color bars in the figure. This figure clearly shows the increase in the lipid to protein ratio and CH_2/CH_3 antisymmetric ratio, and the decrease in the olefinic to lipid ratio. These effects were seen to be more profound in inguinal adipose tissue.

In our immunohistological study, we aimed to differentiate brown adipose tissue and white adipose tissue from each other, so transdifferentiation of these tissues could be investigated. Figure 4 shows the general optical microscope images of UCP1-stained gonadal and inguinal adipose tissue sections of the control and obese (BFMI861) male mice in 40X magnification. Our studies revealed mainly three results; increased cell size, decreased UCP1 protein content, and impaired membrane appearance in obese mice lines. UCP1 proteins appeared as reddish pink color in the images. As seen from Figure 4, adipocytes in obese groups had

fewer amounts of UCP1 proteins in comparison with the control groups. When we compared the amount of brown and white adipocytes in the control and obese groups, we have seen that brown adipocytes replaced to white adipocytes significantly in all obese groups especially in BFMI860 and BFMI861 mice lines and this replacement was more dramatic in inguinal adipose tissue.

4. Discussion

In most healthy cases, the subcutaneous adipose tissue is especially responsible for the storage of fat to supply energy fuel to all kind of cells of the organism in the periods of famine. In obesity, since the storage capacity of subcutaneous adipose tissue is limited, excess lipids begin to be stored in visceral adipose tissue and ectopically in other organs. These excess storages certainly affect the lipid metabolism of the adipose tissues. In our study, we found increased lipid amount and lipid/protein ratio, increased levels of triglycerides and cholesterol esters and qualitative changes in lipid acyl chain towards longer length and decreased content of unsaturation in lipid structure for obese male mice lines compared to the control group. Protein metabolism was also found to be affected via decreased protein amount and changes in protein structure in obese lines.

The lipid to protein ratio gives information about change in lipid content in comparison to protein content. Not surprisingly, we obtained an increased lipid/protein ratio in all obese groups compared to the control group. The expansion of visceral adipose tissue and subcutaneous adipose tissue mass in the body is mainly reason of obesity and it generally results in disturbed lipid and glucose metabolism.[55] Since the subcutaneous adipose tissue storage capacity is limited due to the increase in hypertrophy progresses, excess lipids also accumulate in the visceral adipose tissue stores. It has been reported that visceral adipose tissue is more effective on lipid and glucose metabolism, as it is more sensitive to lipolysis

because of being more active, whereas subcutaneous adipose tissue is responsible for being a passive storage depot.[56] In addition, excess deposition of fat in visceral adipose tissue was reported to be more harmful than excess deposition in subcutaneous adipose tissue, because lipolysis of triglycerides from visceral adipose tissue results in the release of free fatty acids into the portal vein, and in turn into liver.[57]

Olefinic/lipid ratio, which is an index of the content of unsaturation in lipid structure, decreased in obese groups compared to the control groups.[38] The changes in unsaturation lipid content could negatively affect structure, stability, and function of membrane.[58] Polyunsaturated fatty acids (PUFAs) are prone to be attacked by free radicals. These reactions lead to lipid peroxidation, causing changes in unsaturated/saturated lipid composition of the membranes. Several studies have suggested a role for visceral adipose tissue accumulation in the pathogenesis of insulin resistance.[59] Thus, excess deposition of this type adipose tissue has been associated with decreased sensitivity of glucose uptake to insulin stimulation. This association can be also due to the reduced rate of free fatty acid (FFA) reesterification, and increased resistance of lipolysis to the inhibitory effect of insulin in both visceral and peripheral adipocytes.[60-63]

A higher CH_2 antisymmetric stretching/CH_3 antisymmetric stretching ratio demonstrates the qualitatively longer hydrocarbon acyl chain length of lipids. All obese groups showed significantly increased CH_2 to CH_3 antisymmetric stretching ratio, which implies the synthesis of qualitatively longer hydrocarbon acyl chain in biological membranes.[21,39] The changes in lipid hydrocarbon chain length would produce changes in bilayer thickness, which could in turn produce undesirable changes in the thermodynamic stability and passive permeability of the lipid bilayer of biological membranes. Consistently, in our immunohistological staining results, we obtained impaired membrane appearance in adipose tissue cells of obese groups (Figure 4).

Carbonyl/lipid ratio indicates the levels of triglycerides and cholesterol esters in the system.[49,50,64] We obtained a significant increase in the carbonyl/lipid ratio within the adipose tissues of the BFMI860 and BFMI861 lines, especially in inguinal adipose tissue, suggesting an increased concentration of the ester groups belonging to triglycerides in adipose tissues of the obese groups.[49,65] Inguinal adipose tissue, a subcutaneous adipose tissue, demonstrated higher carbonyl/lipid ratio than gonadal adipose tissue, a visceral adipose tissue. The results are in agreement with the other studies in the literature which state that larger adipocytes which consists of subcutaneous adipose tissue, synthesize more triglycerides than smaller adipocytes constituting visceral adipose tissue.[66,67] The storage of triglycerides and lipids within adipose tissue in all obese lines is positively correlated with the markers of insulin resistance.[68,69] The excess release of free fatty acids arises from excess lipolysis of triglycerides. The free fatty acids (FFAs) secreted at high quantities by enlarged adipocytes play a critical role in the development of insulin resistance.[70] Since insulin is the main regulator of hormone sensitive lipase (HSL), the rate controlling enzyme for triglyceride hydrolysis, the inhibitory effect of FFAs on insulin sensitivity leads to enhanced lipolysis in adipocytes.[71] The adipose tissue dysfunction has a critical role in abdominal obesity in vascular risk and risk of developing type 2 diabetes mellitus.[72]

Adipocytes have a special ability to store large quantities of lipids that can be rapidly released and used for energy by other organs when necessary; however, excessive adipose tissue, especially in the visceral adipose tissue depot, is linked with increased risk of insulin resistance, cardiovascular disease and cancer.[73,74]

These changes in membrane lipids and lipid metabolism of adipose tissues also affect the protein metabolism of tissues in obese mice lines. Decreased protein amount calculated from the area value of the amide I band and the area ratios of amide I/ amide I + amide II bands in obese lines imply changes in obesity-induced protein expression. In addition, the decrease in

amide I/amide II ratio, and the shifting of amide I wavenumber to higher values indicate possible obesity-induced alterations in protein structure and conformation.[40]

There are several studies reported increased and decreased expression of proteins including leptin, TNF-α, IL-6 and adiponectin, IL-10, omentin, respectively in WAT adipose tissues.[70,75,76] These proteins were measured in circulation since they were given to the circulatory system after the secretion from adipocytes.[77] However, except adiponectin which is expressed only from WAT adipocytes, these proteins are also expressed from other tissues and circulating cells such as hypothalamus, myocytes, hepatocytes, macrophages and fibroblasts.[76,77] Thus, among the proteins expressed in adipocytes, only the circulating levels of adiponectin can be used to get information for the changes in protein amount in adipose tissues. Together with the decrease in UCP1 protein (Figure 4), decrease in adiponectin protein expression may cause a decrease in the amount of protein in adipose tissues as seen from FTIR results (Table 2 and Figure 2).

Previous studies have shown that increased mass of adipose tissue was found to be correlated with the decreased relative total protein content.[78] As a result of our immunohistological staining, we obtained higher amount of white adipocytes in the obese groups than the control group (Figure 4). This can be explained by two ways, the first one is by an increase of size and number of white adipocytes. Increased white adipose tissue mass in metabolically active sites activates an inflammatory process,[68] and this process creates a strong increase of proinflammatory cytokines, hormone-like molecules and other inflammatory markers, defined as “adipokines” in circulating mechanism.[80,81] This complex physiological reaction progress leads to an increased level of glucocorticoids, induce the development and differentiation of preadipocytes, resulting in an increase of white adipose tissue mass.[82,83] The second and more powerful explanation can be the possibility of the transdifferentation of brown adipocytes into white adipocytes. Accordingly, in our immunohistological staining results, we observed lower

amount of UCP1 proteins in obese groups, implying a decreased amount of brown adipocytes especially in subcutaneous adipose tissue. Their cohabitation could be explained by reversible physiological transdifferentiation because they can be converted to each other, if it is necessary. This capability is so crucial because, the brown adipose tissue is directly associated with resistance to obesity and the brown phenotype exerts an anti-obesity effect.[10] Accordingly, it has been reported that obesity-prone mice have less brown adipose tissue than obesity-resistant mice.[84] It has been also suggested that visceral white adipocytes were actually brown adipocytes previously, some of which turn into white adipocytes because of the smaller size of visceral adipocytes and the different resistance to death of visceral and subcutaneous adipocytes.[10]

Brown adipocytes have also an important role in glucose metabolism and insulin sensitivity. These properties make brown adipose tissue a target for the treatment of obesity, diabetes, and other metabolic disorders.[85] A recent rodent study utilizing brown adipose tissue transplantation from donor mice into the visceral cavity of recipient mice, achieved to increase brown adipose tissue mass, demonstrated improved glucose tolerance, increased insulin sensitivity, reduced body weight, and decreased fat mass.[86] Several studies were able to support brown adipose tissue transplantation experiments and obtained positive treatment results.[87,88] All these data indicate that the brown adipose tissue has very crucial role in obesity and other metabolic diseases.

5. Conclusion

The results of the current study revealed an increased lipid concentration and significantly decreased UCP1 protein content, implying a decrease in brown adipocytes in both adipose tissues of spontaneous obese groups. These results indicated that obese (BFMI) mice lines had a lower amount of brown adipocytes in visceral and subcutaneous adipose tissues, which is an

inclination for obesity. Moreover, the decreased unsaturation ratio, the qualitatively longer hydrocarbon acyl chain length of lipids and the increased amount of triglycerides revealed by FTIR microspectroscopy indicate that both types of adipose tissues, especially inguinal fat were more prone to lipid peroxidation. It is well known that these kind of structural alterations in biomolecules are strongly correlated with membrane functioning and ion channel kinetics.[89,90] Obesity-related structural alterations in lipids and proteins of the BFMI lines, especially for BFM861 line, may be an indicator of a tendency for insulin resistance, therefore type 2 diabetes, besides obesity. One important finding of the study is that both visceral and dominantly subcutaneous adipose tissues demonstrated considerable obesity-induced alterations, therefore both of them take role in the progression of obesity. Furthermore, the current study clearly revealed the power of FTIR microspectroscopy in the precise determination of spectral variations in adipose tissue components of spontaneous mice models.

Acknowledgement

This work was supported by The Scientific and Technological Research Council of Turkey (TUBITAK) with a grant number SBAG-110S235. This work was carried out as a part of the COST Action (BM0901)-SYSGENET.

References

1. F. Zhou, J. F. Fu, C. L. Wang, L. Liang and Z.Y. Zhao, *Zhonghua Liu Xing Bing Xue Za Zhi*, 2007, **28**, 9, 910-913.

2. WHO website, http://www.who.int/mediacentre/factsheets/fs311/en, (accessed October 2014).

3. C. M. Kastorini, H. J. Milionis, K. Esposito, D. Giugliano, J.A. Goudevenos and D.B.

Panagiotakos, *J. Am. Coll. Cardiol*., 2011, **57,** 1299–1313.

4. G. I. Schulman, *J. Clin. Invest*., 2000, **106**, 171-176.

5. R. H. Unger and L. Orci, *FASEB J*., 2001, **15**, 312-321.

6. J. E. Schaffer, *Curr. Opin. Lipidol*., 2003, **14**, 3, 281-287.

7. S. Cinti, *Prostaglandins Leukot. Essent. Fatty Acid*, 2005, **73**, 9-15.

8. E. E. Kershaw and J. S. Flier, *J. Clin. Endocrinol. Metab.*, 2004, **89**, 2548-2556.

9. C.H. Saely, K. Geiger and H. Drexel, *Gerontology*, 2010, **58**, 1, 15-23.

10. S. Cinti, *Am. J. Physiol Endocrinol. Metab.*, 2009, **297**, 977–986.

11. B. Cannon and L. Nedergaard, *Physiol. Rev.*, 2004, **84,** 277-359.

12. S. Klaus, L. Casteilla, F. Bouillaud and D. Ricquier, *Int. J. Biochem.*, 1991, **23**, 791-801.

13. B. Cannon, A. Hedin and J. Nedergaard, *FEBS Lett.*, 1982, **150,** 129-132.

14. S. Cinti, *Nutr. Metab. Cardiovasc. Dis.*, 2006, **16,** 569-574.

15. S. Cinti, *Int. J. Pediatr. Obes.* Suppl., 2008, **2**, 21-26.

16. R. Cancello, M. C. Zingaretti, R. Sarzani, D. Ricquier and S. Cinti, *Endocrinology*, 1998, **139,** 4747-4750.

17. J. W. Bortolotto, C. Reis, A. Ferreira, S. Costa, C. C. Mottin, A. A. Souto and R. M. Guaragna, *Obesity Surgery*, 2005, **15,** 1265-1270.

18. A. Dogan, P Lasch, C. Neuschl, M.K. Millrose, R. Alberts, K. Schughart, D. Naumann and G.A. Brockmann, *BMC Genomics*, 2013, **14**, 386.

19. D. S. Lester, L. H. Kidder, I. W. Levin and E. N. Lewis, *Cell Mol. Biol.*, 1998, **44**, 29-38.

20. K. Z. Liu, A. Man, R. A. Shaw, B. Liang, Z. Xu and Y. Gong, *Biochim. Biophys. Acta.*, 2006, **1758**, 960-967.

21. G. Cakmak, L.M. Miller, F. Zorlu and F. Severcan, *Arch. Biochem. Biophys.*, 2012, **520,** 67-73.

22. O. Bozkurt, S. Haman Bayari, M. Severcan, C. Krafft, J. Popp and F. Severcan, *J.*

Biomed. Opt., 2012, **17**, 7, 076023.

23. J. Kneipp, M. Beekes, P. Lasch and D. Naumann, *J. Neurosci*, 2002, **22**, 8, 2989-2997.

24. A. Marcelli, A. Cricenti, A. Kwiatek and C. Petibois. *Biotechnol. Adv.*, 2012, **30,** 6, 1390-1404.

25. A. Wagener, A. O. Schmitt, S. Aksu, W. Schlote, C. Neuschl and G. A. Brockmann, *Physiol .Genomics*, 2006, **27**, 264-270.

26. A. Hantschel, A. Wagener, C. Neuschl, D. Teupser and G. A. Brockmann, *Obesity Facts*, 2011, **4**, 270-277.

27. R. S. Hageman, A. Wagener, C. Hantschel, K. L. Svenson, G. A. Churchill and G.A. Brockmann, *Physiol. Genomics*, 2010, **42**, 55-66.

28. K. L. Svenson, R. von Smith, P. A. Magnani, H. R. Suetin, B. Paigen, J. K. Naggert, R. Li, G. A. Churchill and L. L. Peters, *J. Appl. Physiol.*, 2007, **102**, 2369-2378.

29. X. Bi, G. Li, S. B. Doty and N. P. Camacho, *Osteoarthritis Cartilage.* 2005, **13,** 12, 1050-1058.

30. P. A. West, M. P. G. Bostrom, P. A. Torzilli and N. P. Camacho, *Applied Spectroscopy*, 2004, **58,** 4, 376-381.

31. A. L. Boskey, M. Goldberg, A. Kulkarni and S. Gomez, *Biochimica et Biophysica Act*, 2006, **1758**, 942–947.

32. A. Dogan, K. Ergen, F. Budak and F. Severcan, *Appl. Spectrosc*., 2007, **61**, 2, 199-203.

33. I. W. Levin and R. Bhargava, *Annu. Rev. Phys. Chem.*, 2005, **56,** 429-474.

34. R. Gasper, J. Dewelle, R. Kiss, T. Mijatovic and E. Goormaghtigh, *Biochim. Biophys .Acta.*, 2009, **1788**, 1263-1270.

35. D. Naumann, in *Infrared and Raman Spectroscopy of Biological Materials*, ed. H. U. Gremlich and B. Yan, Marcel Dekker, New York, vol. 24, ch. 9, pp. 323-379.

36. D. Naumann, H. Fabian and P. Lasch, in *Biological and Biomedical Infrared*

Spectroscopy, ed. A. Barth and P.I. Haris, IOS Press, Netherlands, ch. 12, pp 312-357, 2009.

37. N. S. Ozek, S. Tuna, A. E. Erson-Bensan and F. Severcan, *Analyst*, 2010, **135,** 12, 3094-3102.

38. J. Kneipp, P. Lasch, E. Baldauf, M. Beekes and D. Naumann, *Biochim. Biophys. Acta.*, 2000, **1501**, 189-199.

39. Q. Wang, W. Sanad, L.M. Miller, A. Voigt, K. Klingel, R. Kandolf, K. Stangl and G. Baumann, *Vib. Spectrosc.*, 2005, **38**, 217-222.

40. O. Bozkurt, M. Severcan and F. Severcan, *Analyst*, 2010, **135**, 3110-3119.

41. K.P. Ishida and P.R. Griffiths, *Appl. Spectrosc.*, 1993, **47**, 584-589.

42. M. M. Ibrahim, *Obes. Rev*., 2010, **11**, 1, 11-18.

43. G. Cakmak, F. Zorlu, M. Severcan and F. Severcan, *Anal. Chem*, 2011, **83**, 7, 2438-2444.

44. P. Yu, D. Kevin and L. J. Dasen, *Agric. Food Chem.*, 2008, **56**, 3417–3426.

45. M. Schmidt, T. Wolfram, M. Rumpler, C. P. Tripp and M. Grunze, *Biointerphases*, 2007, **2**, 1–5.

46. Y. Adigüzel, P. I. Haris and F. Severcan, in *Vibrational Spectroscopy in Diagnosis and Screening*, ed. F. Severcan and P. I. Haris, IOS Press, Netherlands ,2012, ch. 3, pp.72-78

47. G. Cakmak, I. Togan and F. Severcan, Aquat Toxicol., 2006, **77**, 1, 53-63.

48. P.I. Haris and F. Severcan, *J. Mol. Catal. B: Enzym*, 1999, **7**, 207–221.

49. M. Nara, M. Okazaki and H. Kagi, *Chem. Phys. Lipids*, 2002, **117**, 1-6.

50. G. Voortman, J. Gerrits, M. Altavilla, M. Henning, L. van Bergeijk and J. Hessels, *Clin. Chem. Lab. Med.*, 2002, **40**, 795-798.

51. S. Kumar, T. S. Shabi and E. Goormaghtigh, PLoS ONE, 2014, **9**, 11, DOI: 10.1371/journal.pone.0111137.

52. A. Derenne, O. Vandersleyen and E. Goormaghtigh, Biochim *Biophys Acta*., 2014, **1841**, 8, 1200-1209.

53. B. L. Smiley and G. L. Richmond., *J. Phys. Chem. B*, 1999, **103**, 4, 653–659.

54. K. M. Antoine, S. Mortazavi, A. D. Miller and L. M. Miller, *J Forensic Sci.*, 2010, **55**, 2, 513-518.

55. H. E. Bays, J. M. Gonzalez-Campoy, G. A. Bray, A. E. Kitabchi, D.A. Bergman, A. B. Schorr, H. W. Rodbard and R. R. Henry, *Expert. Rev. Cardiovasc. Ther.*, 2008, **6**, 3, 343-368.

56. E. Bonora, S. Del Prato, R. C. Bonadonna, G. Gulli, A. Solini and M. L. Shank, *Diabetes*, 1992, **41**, 9, 1151-1159.

57. P. Bjorntorp, *Arteriosclerosis*, 1990, **10**, 493-496.

58. R. N. A. H. Lewis and R. N. McElhaney, in *The Structure of Biological Membranes*, ed. P. L. Yeagle, CRC Press, New YORK, 3rd edn, 2011, ch. 4 , pp 29-36.

59. Y. Gastaldelli, M. Miyazaki, M. Pettiti, S. Matsuda, E. Mahankali, R.A. Santini DeFronzo and E.J. Ferrannini, *Clin. Endocrinol. Metab*., 2002, **87**, 11, 5098-5103.

60. M. Broche, R. D. Starling, A. Tchernof, D. E. Matthews, E. Garcia-Rubi and E. T. Poehlman, *J. Clin. Endocrinol. Metab.*, 2000, **85**, 2378–2384.

61. J. R. Zierath, J. N. Livingston, A. Thorne, J. Bolinder, S. Reynisdottir, F. Lonnqvist and P. Arner, *Diabetologia*, 1998, **41**, 1343–1354.

62. S. E. Meek, K. S. Nair and M. D. Jensen, *Diabetes,* 1999, **48**, 10–14.

63. J. B. Albu, M. Curi, M. Shur, L. Murphy, D.E. Matthews and F. X. Pi-Sunyer, *Am. J. Physiol.*, 1999, **277,** 551-560.

64. N. S. Ozek, Y. Sara, R. Onur and F. Severcan, *Biosci. Rep.*, 2010, **30**, 41-50.

65. G. Cakmak, I. Togan, C. Uguz and F. Severcan, *Appl. Spectrosc.,* 2003, **57**, 835-841.

66. N. K. Edens, S. K. Fried, J. G. Kral, J. Hirsch and R. L. Leibel, *Am. J. Physiol.*, 1993, **265,** 374-379.

67. C. Farnier, S. Krief, M. Blache, F. Diot-Dupuy, G. Mory, P. Ferre and R. Bazin, *Int. J.*

Obes. Relat. Metab. Disord., 2003, **27**, 1178- 1186.

68. D. A. Pan, S. Lillioja, A. D. Kriketos, M. R. Milner, L. A. Baur, C. Bogardus, A. B. Jenkins and L. H. Storlien, *Diabetes*, 1997, **46**, 983-988.

69. D. I. Phillips, S. Caddy, V. Ilic, B. A Fielding, K. N Frayn, A. C Borthwick and R. Taylor, *Metabolism*, 1996, **45**, 947-950.

70. G. S. Hotamisligil, P. Arner, J. F. Caro, R. L. Atkinson and B. M. Spiegelman, *J. Clin. Invest*., 1995, **95**, 2409–2415.

71. H. Ruan, N. Hacohen, T. R. Golub, L. van Parijs and H. F. Lodish, *Diabetes*, 2002, **51**, 1319–1336.

72. G. R. Hajer, T.W. van Haeften and F. L. J. Visseren, *European Heart Journal*, 2008, **29**, 2959–2971.

73. P. Hossain, B. Kawar and M. El Nahas, *N. Engl. J. Med.*, 2007, **356,** 213–215.

74. D.H. Cohen and D. Leroith, *Endocr. Relat. Cancer*, 2012, **19**, 27–45.

75. M. Qatanani and M. A. Lazar, *Genes Dev.*, 2007, **21**, 12, 1443-1455.

76. K. Makki, P. Froguel and I. Wolowczuk, *ISRN Inflamm.*, 2013, DOI:10.1155/2013/139239.

77. M. K. Piya, P. G. McTernan and S. Kumar, *J Endocrinol.* 2013, **216**, 1, T1-T15.

78. P. M. Seraphim, M. T. Nunes and U. F. Machado, *Braz. J. Med. Biol. Res*., 2001, **34**, 10, 1353-1362.

79. R. Cancello and K. Clément, *International Journal of Obstetrics & Gynaecology*, 2006, **113**, 10, 1141–1147.

80. F. Lago, C. Dieguez, J. Gómez-Reino and O. Gualillo, *Nature Clinical Practice Rheumatology*, 2007, **3**, 12, 716–724.

81. S. E. Wozniak, L. L. Gee, M. S. Wachtel and E. E. Frezza, *Digestive Diseases and Sciences*, 2009, **54**, 9, 1847–1856.

82. J. Q. Purnell, S. E. Kahn, M. H. Samuels, D. Brandon, D. L. Loriaux and J. D. Brunzell, *American Journal of Physiology*, 2009, **296**, 2, 351–357.

83. V. Bourlier, A. Zakaroff-Girard and A. Miranville, *Circulation*, 2008, **117**, 6, 806–815.

84. K. Almind, M. Manieri, W. I. Sivitz, S. Cinti and C. R. Kahn, *Proc. Natl. Acad. Sci.*, 2007, **104,** 2366–2371.

85. K. L. Townsend and Y. H. Tseng, *Adipocyte*, 2012, **1**, 13–24.

86. K. I. Stanford, R. J. W. Middelbeek, K. L. Townsend, D. An, E. B. Nygaard, K. M. Hitchcox, K. R. Markan, K. Nakano, M. F. Hirshman, Y. Tseng and L. J. Goodyear, *J. Clin. Invest*., 2013, **123**, 215–223.

87. S. C. Gunawardana and D. W. Piston, *Diabetes*, 2012, **61**, 674–682.

88. X. Liu, Z. Zheng, X. Zhu, M. Meng, L. Li, Y. Shen, Q. Chi, D. Wang, Z. Zhang, C. Li, Y. Li, Y. Xue, J.R. Speakman and W. Jin, *Cell Res.*, 2013, **23**, 851–854.

89. A. A. Spector and M. A. Yorek, *J. Lipid Res.*, 1985, **26**, 9, 1015-1035.

90. M. S. Awayda, W. Shao, F. Guo, M. Zeidel and W. G. Hill, *J. Gen. Physiol.*, 2004, **1238**, 6, 709-727.

Table 1. General band assignment of FTIR spectrum of an adipose tissue.[18,35,36]

Band No	Wavenumber (cm-1)	Definition of the spectral assignment
1	3290	N–H and O–H stretching: Mainly N–H stretching (amide A) of proteins with the little contribution from O–H stretching of polysaccharides, carbohydrates and water
2	3005	Olefinic=CH stretching vibration: unsaturated lipids, cholesterol esters
3	2957	CH_3 anti-symmetric stretching: lipids, protein side chains, with some contribution from carbohydrates and nucleic acids
4	2924	CH_2 anti-symmetric stretching: mainly lipids, with some contribution from proteins, carbohydrates, nucleic acids
5	2875	CH_3 symmetric stretching: mainly protein side chains, with some contribution from lipids, carbohydrates and nucleic acids
6	2855	CH_2 symmetric stretching: mainly lipids, with some contribution from proteins, carbohydrates, nucleic acids
7	1744	Carbonyl C=O stretch: triglycerides
8	1654	Amide I (protein C=O stretching)
9	1545	Amide II (protein N-H bend, C-N stretch)

Table 2. The band area and band position values of the amide I band in male control (DBA/2J) and obese (BFMI lines) mice gonadal and inguinal adipose tissues.

		Control	BFMI852	BFMI856	BFMI860	BFMI861
Amide I area value	Gonadal	0.83±0.01	0.63±0.04*	0.42±0.03*	0.38±0.02**	0.37±0.03**
	Inguinal	0.73±0.04	0.57±0.05	0.56±0.02	0.33±0.04**	0.29±0.01**
Amide I band position	Gonadal	1652.56±0.30	1653.50±0.13*	1654.53±0.51*	1655.31±0.25**	1656.65±0.60**
	Inguinal	1652.93±0.93	1653.31±0.42*	1654.57±0.18**	1656.85±0.29**	1656.94±0.28**

*The values are the mean ± standard error of the mean for each group. Comparison was performed by one-way ANOVA and Tukey's test was used as a post test. The degree of significance was denoted with * for the comparison of control DBA/J2 strain with other BFMI lines. P values less than or equal to 0.05 were considered as statistically significant; *p ≤ 0,05; **p ≤ 0,01; ***p ≤ 0,001.*

Table 1S. The spectral regions and baseline points for particular infrared bands used in calculation of band area ratios.

Infrared band	**Integrated spectral region (cm^{-1})**	**Baseline points (cm^{-1})**
Olefinic=CH	3020-2992	3100-2740
CH_3 antisymmetric stretching	2976-2948	3100-2740
CH_2 antisymmetric stretching	2940-2916	3100-2740
CH_3 symmetric stretching	2880-2864	3100-2740
CH_2 symmetric stretching	2864-2844	3100-2740
C–H region	2980-2830	3100-2740
Carbonyl (C = O) stretching	1764-1724	1850-1500
Amide I	1672-1636	1850-1500
Amide II	1560-1536	1850-1500

Legends of Figures

Figure 1. Representative FTIR spectra of IF adipose tissue of male control DBA/J2 and obese BFMI861 line in the 4000-750 cm^{-1} region.

Figure 2. The bar graphs of the lipid/protein, CH_2 symmetric/CH_2 antisymmetric, CH_2/CH_3 antisymmetric, olefinic/lipid, carbonyl/lipid, CH_2 antisymmetric/lipid, amide I/ amide II, amide I/ amide I + amide II ratios of control (DBA/J2) and 4 different obese (BFMI) male mice lines (n=6 for each line). The degree of significance was denoted by * for the comparison of control DBA/J2 line with BFMI lines as: $*p < 0.05$, $**p < 0.01$,$***p < 0.001$ and by $^{+}$ for the comparison of gonadal adipose tissue with inguinal adipose tissue in same line as: $^{+}p < 0.05$, $^{++}p < 0.01$,$^{+++}p < 0.001$.

Figure 3. The representative spectral maps of lipid/protein, olefinic/protein and CH_2/CH_3 antisymmetric ratios belong to inguinal adipose tissue of control (DBA/J2) and obese (BFMI861) male mice line. The absorbance in the spectral maps was represented in color-coded images, where low absorption was represented in blue and high absorption was represented in red color.

Figure 4. Immunohistological UCP1 staining results of gonadal and inguinal adipose tissues which belong to the control and obese (BFMI861) male mice. Microscopic images of Gonadal adipose tissue of control group (A), inguinal adipose tissue of the control group (B), gonadal adipose tissue of the obese group (C), inguinal adipose tissue of the obese group (D) in 40X magnification. The regions which are shown by arrows are brown adipose tissue and the rest of the cells belong to white adipose tissue.

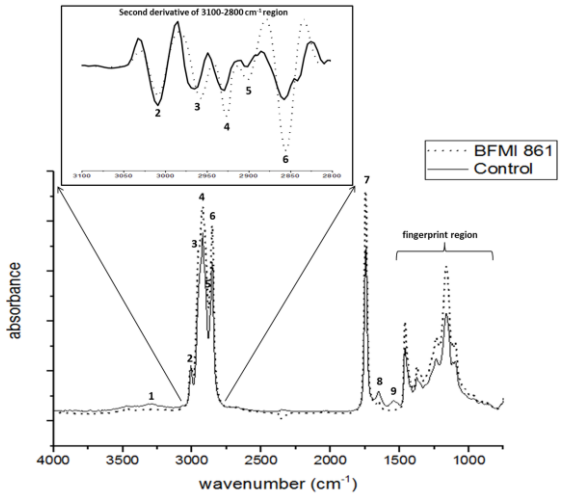

Figure 1

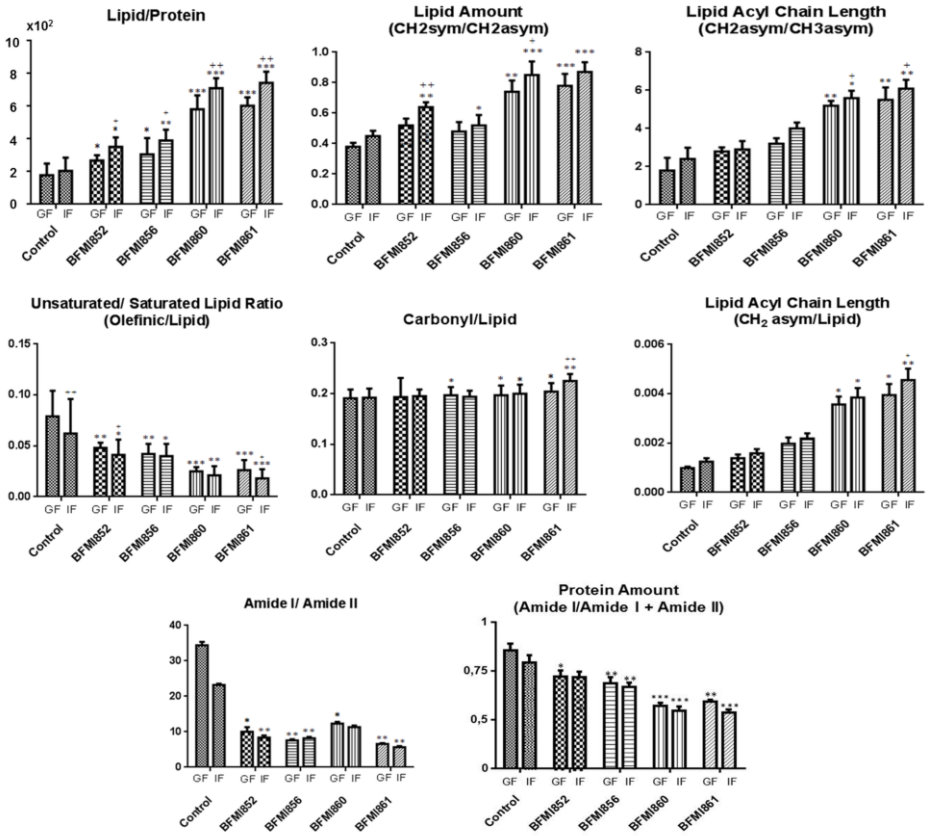

Figure 2

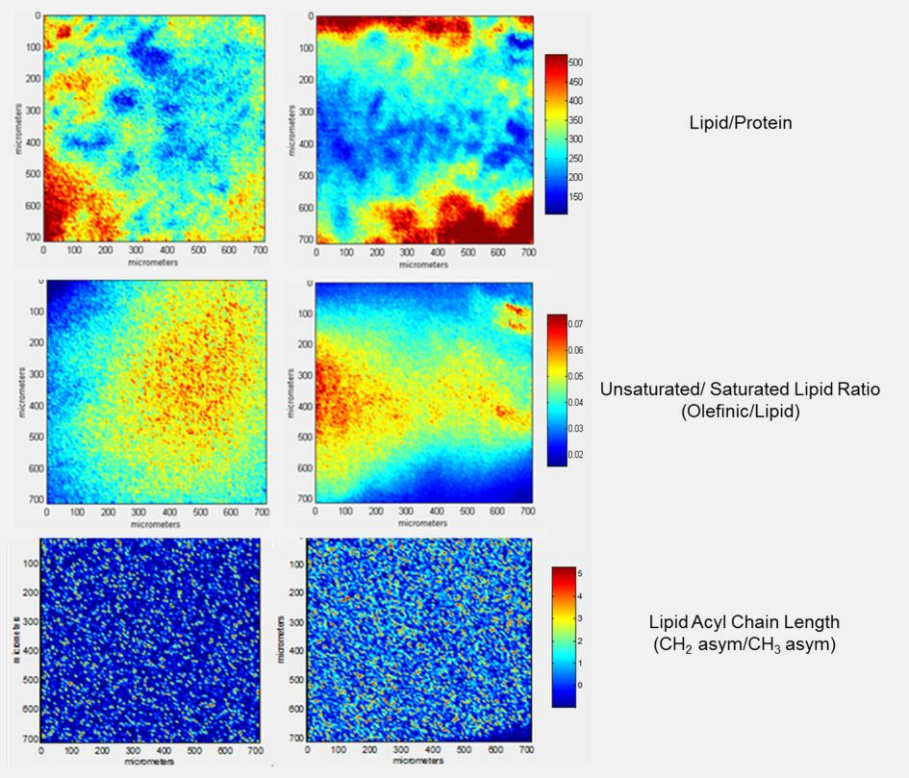

Figure 3

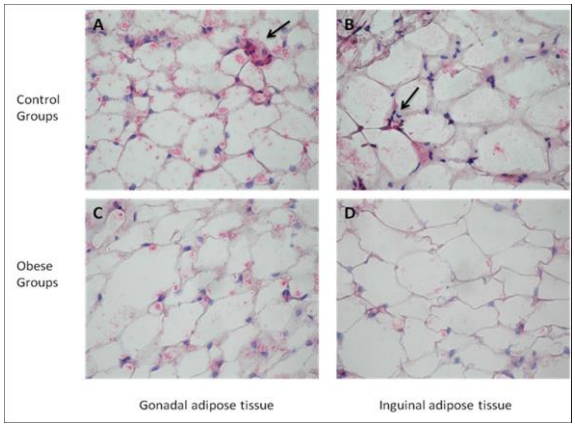

Figure 4

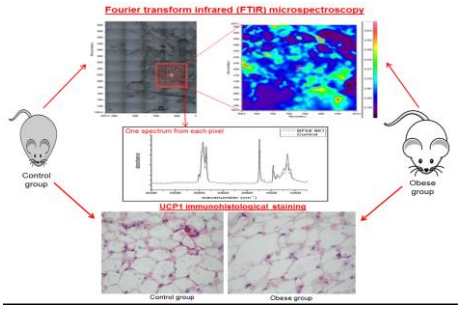

Graphical Abstract

Textual abstract

FTIR microspectroscopy coupled with UCP1 immunohistological staining enable to detect obesity-related molecular alterations and transdifferentiation in visceral and subcutaneous adipose tissues in spontaneous obese mice lines.